Inorg. Chem. **2007**, *46*, 7571–7578

Layered Cobalt(II) and Nickel(II) Diphosphonates Showing Canted Antiferromagnetism and Slow Relaxation Behavior

Deng-Ke Cao,[†] Yi-Zhi Li,[†] and Li-Min Zheng*[,†,‡]

State Key Laboratory of Coordination Chemistry, Coordination Chemistry Institute, School of Chemistry and Chemical Engineering, Nanjing University, Nanjing 210093, P. R. China, and State Key Laboratory of Structure Chemistry, Fujian Institute of Research on the Structure of Matter, The Chinese Academy of Sciences, Fuzhou 350002, P. R. China

Received June 4, 2007

Reactions of 2-(1-imidazole)-1-hydroxyl-1,1′-ethylidenediphosphonic acid ($ImhedpH_4$) and cobalt or nickel salts under hydrothermal conditions lead to four new metal phosphonates with two types of structures: $M_3(ImhedpH)_2(H_2O)_4 \cdot 2H_2O$ [M = Co(II) (**1**) and Ni(II) (**2**)] and $M(ImhedpH_3)_2(H_2O)_2$ [M = Co(II) (**3**) and Ni(II) (**4**)]. Compounds **1** and **2** are isostructural and show a layered structure made up of $M_3(ImhedpH)_2(H_2O)_4$ trimer units. These trimers are connected by edge-sharing of the $\{Co(2)O_6\}$ octahedra, forming an undulating chain. The adjacent chains are fused through the coordination of the phosphonate oxygen atom from one chain to the Co(2) atom of the other, thus generating a two-dimensional layer containing 4-, 8-, and 16-membered rings. The imidazole groups are grafted on the two sides of the layer. Compounds **3** and **4** are also isostructural and show a mononuclear structure with extensive hydrogen bond interactions. Magnetic measurements reveal that both **1** and **2** exhibit canted antiferromagnetism at 2.6 and 5.0 K, respectively. Below these temperatures, slow relaxation is observed from the ac susceptibility measurements corresponding to the spin-glass-like behaviors.

Introduction

Layered metal phosphonates are considered a very large and versatile class of layered materials in which many different geometrical arrangements can be realized by an appropriate choice of the layered structure and/or the organic group.[1,2] In some cases, a slight modification of the ligand and/or the reaction condition is sufficient to alter the structure and hence the magnetic properties. For example, a few cobalt diphosphonates with layered structures have been reported based on methylenediphosphonate and its derivatives (Scheme 1).

The reaction of cobalt salt with methylenediphosphonic acid ($mdpH_4$) result in a layered compound $Na_2Co(O_3PCH_2PO_3)\cdot H_2O$[3] where the CoO_5 square pyramids are corner-shared with the CPO_3 tetrahedra forming a layer containing 12-membered rings. The use of aminomethylenediphosphonic acid ($amdpH_4$) affords $NaCo_2\{NH_3CH(PO_3)(PO_3H_{0.5})\}_2(H_2O)_2\cdot xH_2O$[4] in which the CoO_6 octahedra and CPO_3 tetrahedra are connected through vertex-sharing, forming a layer containing 8- and 16-membered rings. When 1-aminoethylidenediphosphonic acid ($aedpH_4$) is used, compound $Co_3\{CH_3C(NH_3)(PO_3H)(PO_3)\}_2\{CH_3C(NH_3)(PO_3H)_2\}_2(H_2O)_4\cdot 2H_2O$[5] is obtained where corner-sharing CoO_6 octahedra and CPO_3 tetrahedra lead to a two-dimensional layer containing 24-membered rings. The use of 1-hydroxyethylidenediphosphonate ($hedpH_4$) produces $Na_6Co_7(hedp)_2(hedpH)_4(H_2O)_4\cdot 8H_2O$,[6] which bears a layered structure composing of two types of chains: $\{Co_3(hedp)_2\}_n$ (chain I) made up of the CoO_6 octahedra and CPO_3 tetrahedra through corner-sharing and $\{Co_2(hedpH)_2\}_n$ (chain II) containing edge-shared CoO_6 octahedra bridged by $hedpH^{3-}$ groups. The magnetic properties of the former three compounds are simply paramagnetic with dominant antiferromagnetic interactions between the

* To whom correspondence should be addressed. E-mail: lmzheng@nju.edu.cn. Fax: +86-25-83314502.
† Nanjing University.
‡ The Chinese Academy of Sciences, Fuzhou.

(1) Alberti, G. In *Comprehensive Supramolecular Chemistry*; Atwood, J. L., Davies, J. E. D., MacNicol, D. D., Vogtle, F., Eds.; Pergamon Press: New York, 1996; Vol. 7, p 151.
(2) Clearfield, A. *Prog. Inorg. Chem.* **1998**, *47*, 371−510.
(3) Distler, A.; Lohse, D. L.; Sevov, S. C. *J. Chem. Soc., Dalton Trans.* **1999**, 1805.
(4) Bao, S.-S.; Zheng, L.-M.; Liu, Y.-J.; Xu, W.; Feng, S. *Inorg. Chem.* **2003**, *42*, 5037.
(5) Yin, P.; Wang, X.-C.; Gao, S.; Zheng, L.-M. *J. Solid State Chem.* **2005**, *178*, 1049.
(6) Yin, P.; Gao, S.; Zheng, L.-M.; Wang, Z.; Xin, X.-Q. *Chem. Commun.* **2003**, 1076.

10.1021/ic701098t CCC: $37.00
Published on Web 08/09/2007

Scheme 1

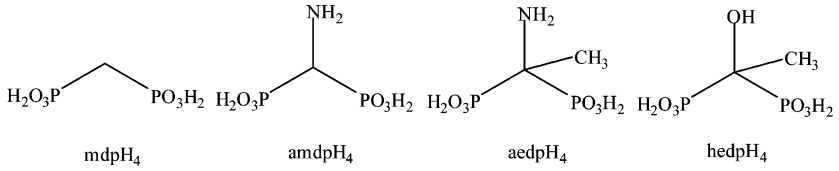

Scheme 2

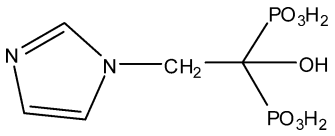

magnetic center, while the latter compound experiences a two-step magnetic phase transition in the field range 0−70 kOe, corresponding to a metamagnetic transition from an antiferromagnetic state to a ferrimagnetic state followed by the transition from a ferrimagnetic state to a ferromagnetic state.

To explore new metal diphosphonate materials with novel types of layer structures, we employ the 2-(1-imidazole)-1-hydroxyl-1,1′-ethylidenediphosphonic acid [ImhedpH$_4$, (1-$C_3H_3N_2$)$CH_2C(OH)(PO_3H_2)_2$] (Scheme 2) where the imidazole group is introduced to hedpH$_4$. ImhedpH$_4$ is also called zoledronic acid and has been widely investigated as a third-generation bisphosphonate drug for treating diseases associated with increased bone resorption.[7] As far as we are aware, no metal−Imhedp compound has been reported in the literature except $Na^+ \cdot C_5H_9N_2O_7P_2^- \cdot 4H_2O$.[8] In this paper, we report four compounds based on zoledronic acid with formula $M_3(ImhedpH)_2(H_2O)_4 \cdot 2H_2O$ [M = Co(**1**), Ni (**2**)], and $M(ImhedpH_3)_2(H_2O)_2$ [M = Co (**3**), Ni (**4**)]. Both compounds **1** and **2** exhibit a new type of layer structure and show weak ferromagnetism and spin-glass-like behaviors at low temperature.

Experimental Section

Materials and Methods. 2-(1-imidazole)-1-hydroxyl-1,1′-ethylidenediphosphonic acid (ImhedpH$_4$) was prepared according to the literature.[9] All other starting materials were purchased as reagent-grade chemicals and used without further purification. Elemental analyses were performed on a Perkin-Elmer 240C elemental analyzer. The IR spectra were obtained as KBr disks on a VECTOR 22 spectrometer. Magnetic susceptibility data were obtained on microcrystalline samples (9.87 mg for **1** and 18.49 mg for **2**), using a Quantum Design MPMS-XL7 SQUID magnetometer. Diamagnetic corrections were made for both the sample holder and the compound estimated from Pascal's constants.[10]

Preparation of $Co_3(ImhedpH)_2(H_2O)_4 \cdot 2H_2O$ (1). A mixture of ImhedpH$_4$ (0.10 mmol, 0.0272 g) and $Co(CH_3CO_2)_2 \cdot 4H_2O$ (0.10 mmol, 0.0249 g) in 8 mL of H_2O, adjusted to pH = 4.49 with 1 M NaOH, was kept in a Teflon-lined autoclave at 160 °C for 48 h. After slow cooling to room temperature, purple blocky crystals were collected as a monophasic material based on the powder XRD. Yield: 23 mg (56% based on Co). Anal. Found (Calcd) for $C_{10}H_{26}N_4O_{20}P_4Co_3$: C, 14.42 (14.59); H, 3.06 (3.18); N, 6.68 (6.81). IR (KBr, cm^{-1}): 3426(m, br), 3147(m), 2993(m), 1662(w, br), 1573(m), 1545(w), 1455(w), 1386(w), 1319(vw), 1288(m), 1225-(vw), 1150(vs), 1051(vs), 979(s), 951(m), 926(m), 894(m), 851-(m), 756(w), 711(w), 682(w), 638(m), 604(vw), 577(m), 545(m), 512(w), 481(m), 434(w).

Preparation of $Ni_3(ImhedpH)_2(H_2O)_4 \cdot 2H_2O$ (2). A mixture of ImhedpH$_4$ (0.10 mmol, 0.0272 g) and $Ni(CH_3CO_2)_2 \cdot 4H_2O$ (0.10 mmol, 0.0249 g) in 8 mL of H_2O, adjusted to pH = 4.50 with 1 M NaOH, was kept in a Teflon-lined autoclave at 160 °C for 48 h. After slow cooling to room temperature, green blocky crystals were collected as a monophasic material based on the powder XRD. Yield: 22 mg (54% based on Ni). Anal. Found (Calcd) for $C_{10}H_{26}N_4O_{20}P_4Ni_3$: C, 14.72 (14.60); H, 3.13 (3.19); N, 6.80 (6.81). IR (KBr, cm^{-1}): 3423(m, br), 3148(m), 2994(m), 1654(w, br), 1571(m), 1544(w), 1454(w), 1397(w), 1317(vw), 1289(m), 1225-(vw), 1152(vs), 1053(vs), 982(s), 955(m), 926(w), 893(w), 868-(w), 850(m), 762(w), 712(m), 684(w), 639(m), 607(vw), 581(s), 547(m), 517(w), 484(m), 442(w).

Preparation of $Co(ImhedpH_3)_2(H_2O)_2$ (3). A mixture of ImhedpH$_4$ (0.10 mmol, 0.0272 g) and $CoSO_4 \cdot 7H_2O$ (0.10 mmol, 0.0281 g) in 8 mL of H_2O (pH = 2.80) was kept in a Teflon-lined autoclave at 140 °C for 48 h. After slow cooling to room temperature, purple blocky crystals were collected as a monophasic material based on the powder XRD. Yield: 19 mg (30% based on Co). Anal. Found (Calcd) for $C_{10}H_{22}N_4O_{16}P_4Co$: C, 18.63 (18.85); H, 3.40 (3.48); N, 8.68 (8.79). IR (KBr, cm^{-1}): 3584(s), 3333(s), 3225−2743(m, br), 1855(w), 1645(m), 1579(m), 1545(m), 1459-(w), 1445(m), 1416(w), 1381(w), 1353(w), 1323(w), 1289(m), 1236(m), 1177(s), 1153(vs), 1111(s), 1074(vs), 1047(m), 1017(m), 962(s), 922(s), 898(s), 858(vw), 834(m), 781(vw), 756(m), 715-(m), 677(w), 633(m), 594(m), 557(m), 529(m), 481(s), 411(vw).

Preparation of $Ni(ImhedpH_3)_2(H_2O)_2$ (4). A mixture of ImhedpH$_4$ (0.10 mmol, 0.0272 g) and $NiSO_4 \cdot 6H_2O$ (0.10 mmol, 0.0263 g) in 8 mL of H_2O (pH = 2.72) was kept in a Teflon-lined autoclave at 140 °C for 48 h. After slow cooling to room temperature, light green blocky crystals were collected as a monophasic material based on the powder XRD. Yield: 20 mg (31% based on Ni). Anal. Found (Calcd) for $C_{10}H_{22}N_4O_{16}P_4Ni$: C, 18.74 (18.86); H, 3.59 (3.48); N, 8.66 (8.80)%. IR (KBr, cm^{-1}): 3584(s), 3333(s), 3231−2739(m, br), 1854(w), 1648(m), 1578(m), 1544(m), 1458(w), 1444(w), 1417(w), 1381(w), 1353(w), 1322-(w), 1290(m), 1233(m), 1176(s), 1154(vs), 1112(s), 1075(vs), 1047-(w), 1017(m), 962(s), 922(m), 897(m), 858(w), 836(m), 756(m), 716(m), 678(w), 633(m), 595(m), 560(m), 529(m), 482(s), 412(w).

X-ray Crystallographic Studies. Single crystals of dimensions 0.2 × 0.15 × 0.1 mm for **1**, 0.07 × 0.05 × 0.03 mm for **2**, 0.06 ×

(7) (a) Nancollas, G. H.; Tang, R.; Phipps, R. J.; Henneman, Z.; Gulde, S.; Wu, W.; Mangood, A.; Russell, R. G. G.; Ebetino, F. H. *Bone (San Diego, CA, U.S.)* **2006**, *38*, 617. (b) Widler, L.; Jaeggi, K. A.; Glatt, M.; Müller, K.; Bachmann, R.; Bisping, M.; Born, A.-R.; Cortesi, R.; Guiglia, G.; Jeker, H.; Klein, R.; Ramseier, U.; Schmid, J.; Schreiber, G.; Seltenmeyer, Y.; Green, J. R. *J. Med. Chem.* **2002**, *45*, 3721.
(8) Gossman, W. L.; Wilson, S. R.; Oldfield, E. *Acta Crystallogr.* **2002**, *C58*, m599.
(9) (a) Jiang, Y.; Zhang, X. Q.; Xu, Z. R. *Chin. J. Pharm.* **2004**, *35*(4), 204. (b) Jiang, Y.; Zhang, X. Q.; Xu, Z. R. *Huaxi J. Pharm.* **2005**, *20* (1), 29.
(10) Kahn, O. *Molecular Magnetism*; VCH: New York, 1993.

Table 1. Crystallographic Data and Refinement Parameters for **1**−**4**

compound	**1**	**2**	**3**	**4**
empirical formula	$C_{10}H_{26}N_4O_{20}P_4Co_3$	$C_{10}H_{26}N_4O_{20}P_4Ni_3$	$C_{10}H_{22}N_4O_{16}P_4Co$	$C_{10}H_{22}N_4O_{16}P_4Ni$
fw	823.02	822.36	637.13	636.91
cryst syst	triclinic	triclinic	triclinic	triclinic
space group	$P\bar{1}$	$P\bar{1}$	$P\bar{1}$	$P\bar{1}$
a (Å)	6.945(1)	6.902(2)	7.417(2)	7.387(2)
b (Å)	9.573(2)	9.625(3)	8.433(3)	8.399(2)
c (Å)	9.788(2)	9.699(3)	9.756(3)	9.777(3)
α (deg)	77.284(3)	77.193(7)	105.358(6)	69.330(6)
β (deg)	78.623(4)	78.779(5)	111.757 (6)	67.840(5)
γ (deg)	87.507(4)	87.223(8)	97.075(6)	83.022(6)
V (Å^3)	622.4(2)	616.3(3)	529.6(3)	521.8(2)
Z	1	1	1	1
ρ_{calcd} (g cm^{-3})	2.196	2.216	1.998	2.027
F(000)	415	418	325	326
GOF on F^2	1.055	1.085	1.083	1.039
R1, wR2[a] [$I > 2\sigma(I)$]	0.0476, 0.1185	0.0634, 0.1541	0.0541, 0.1454	0.0553, 0.1420
R1, wR2[a] (all data)	0.0571, 0.1245	0.0817, 0.1596	0.0680, 0.1863	0.0695, 0.1481
$(\Delta\rho)_{max}$, $(\Delta\rho)_{min}$ (e Å^{-3})	0.746, −0.698	0.720, −0.707	0.711, −1.069	0.684, −0.677

[a] $R1 = \sum||F_o| - |F_c||/\sum|F_o|$, $wR2 = [\sum w(F_o^2 - F_c^2)^2/\sum w(F_o^2)^2]^{1/2}$.

0.05 × 0.04 mm for **3**, and 0.08 × 0.06 × 0.05 mm for **4** were used for structural determinations on a Bruker SMART APEX CCD diffractometer (for **1**, **3**, and **4**) or a Bruker SMART 1K CCD diffractometer (for **2**) using graphite-monochromatized Mo Kα radiation ($\lambda = 0.71073$ Å) at room temperature. A hemisphere of data was collected in the θ range of 2.17−26.00° for **1**, 2.19−26.00° for **2**, 2.39−25.00° for **3**, and 2.61−25.00° for **4** using a narrow-frame method with scan widths of 0.30° in ω and an exposure time of 5 s/frame. The numbers of observed and unique reflections are 3282 and 2331 ($R_{int} = 0.0213$) for **1**, 4335 and 2382 ($R_{int} = 0.0274$) for **2**, 2620 and 1826 ($R_{int} = 0.0227$) for **3**, and 2626 and 1801 ($R_{int} = 0.0243$) for **4**. The data were integrated using the Siemens *SAINT* program,[11] with the intensities corrected for Lorentz factor, polarization, air absorption, and absorption due to variation in the path length through the detector faceplate. Multiscan absorption corrections were applied. The structures were solved by direct methods and refined on F^2 by full matrix least squares using *SHELXTL*.[12] All the non-hydrogen atoms were located from the Fourier maps and were refined anisotropically. All H atoms were refined isotropically, with the isotropic vibration parameters related to the non-H atom to which they are bonded. The crystallographic data for the four compounds are listed in Table 1, and selected bond lengths and angles are given in Tables 2−5. CCDC publication nos. 645353−645356 contain the supplementary crystallographic data for this paper.

Results and Discussion

Syntheses. Compounds **1**−**4** were prepared through hydrothermal reactions of $ImhedpH_4$ and the corresponding metal acetates or sulfates at 160 or 140 °C for 2 days. It was found that the reaction temperature and pH value of the reaction mixture, M/ligand molar ratio, and the metal source play key roles in the formation of the final products. Both **1** and **2** can be prepared as pure phases at 160 °C, pH of 4.5−5.0, and with the $M(CH_3CO_2)_2$/ligand molar ratio of (0.8−1):1. When the temperature is lowered to 140 °C or the pH value is beyond the range of 4.5−5.0, only flocculelike materials are obtained. Pure phases of compounds **3** and **4** can be obtained at 140 °C when the pH falls in the range of 2.5−3.0 and the MSO_4/ligand molar ratio is (0.5−1):1. If we use MSO_4 as the starting material in preparing **1** and **2** or $M(CH_3CO_2)_2$ in preparing **3** and **4**, large amounts of the unrecognized flocculelike materials would be obtained. Attempts to synthesize compounds **1** and **2** by using **3** and **4**, respectively, as the starting materials were not successful.

Table 2. Selected Bond Lengths (Å) and Angles (deg) for **1**[a]

Co1−O1	2.070(3)	Co2−O2C	2.062(3)
Co1−O4	2.068(3)	P1−O1	1.523(3)
Co1−O1W	2.144(3)	P1−O2	1.544(3)
Co2−O2	2.114(3)	P1−O3	1.492(4)
Co2−O5	2.126(3)	P2−O4	1.495(3)
Co2−O2W	2.137(4)	P2−O5	1.549(3)
Co2−O7	2.180(3)	P2−O6	1.531(3)
Co2−O6B	2.001(3)	O7−C5	1.448(6)
O1−Co1−O4	91.78(13)	O6B−Co2−O2	174.29(13)
O1−Co1−O1W	87.88(13)	O6B−Co2−O5	98.27(13)
O4−Co1−O1W	90.68(13)	O6B−Co2−O7	91.75(13)
O2−Co2−O5	83.86(13)	O6B−Co2−O2W	93.24(13)
O2−Co2−O7	83.29(12)	O6B−Co2−O2C	97.93(13)
O2−Co2−O2W	84.26(13)	P1−O1−Co1	132.13(19)
O5−Co2−O7	81.66(12)	P1−O2−Co2	114.16(18)
O5−Co2−O2W	167.60(13)	P1−O2−Co2C	152.7(2)
O7−Co2−O2W	93.44(13)	P2−O4−Co1	136.8(2)
O2C−Co2−O2	87.25(13)	P2−O5−Co2	114.94(18)
O2C−Co2−O5	92.27(13)	P2−O6−Co2B	128.50(19)
O2C−Co2−O7	169.25(13)	C5−O7−Co2	103.2(3)
O2C−Co2−O2W	90.68(14)	Co2C−O2−Co2	92.75(12)

[a] Symmetry codes: A, $-x + 2$, $-y$, $-z + 1$; B, $-x + 1$, $-y$, $-z + 2$; C, $-x + 2$, $-y$, $-z + 2$.

Crystal Structures of $M_3(ImhedpH)_2(H_2O)_4 \cdot 2H_2O$ [M = Co(II) (1), Ni(II) (2)]. Compounds **1** and **2** are isostructural, crystallizing in triclinic space group $P\bar{1}$. Figure 1 displays the building unit of **1**. It contains two independent Co atoms with the Co1 atom sitting in an inversion center and Co2 at a general position. Both have a distorted-octahedral geometry. Four equatorial sites around the Co1 atom are occupied by phosphonate oxygens (O1, O4, O1A, and O4A) from two equivalent $ImhedpH^-$ ligands. The remaining two axial sites are filled with two equivalent water molecules (O1W and O1WA). For the Co2 atom, three of its six coordination sites are occupied by O2, O5, and O7

(11) *SAINT*, *Program for Data Extraction and Reduction*; Siemens Analytical X-ray Instruments: Madison, WI, 1994−1996.
(12) *SHELXTL*, *Reference Manual*, version 5.0; Siemens Industrial Automation, Analytical Instruments: Madison, WI, 1997.

Table 3. Selected Bond Lengths (Å) and Angles (deg) for **2**[a]

Ni1−O1	2.051(4)	Ni2−O2C	2.017(4)
Ni1−O4	2.042(4)	P1−O1	1.520(4)
Ni1−O1W	2.094(4)	P1−O2	1.546(4)
Ni2−O2	2.087(4)	P1−O3	1.509(4)
Ni2−O5	2.105(5)	P2−O4	1.505(4)
Ni2−O2W	2.093(4)	P2−O5	1.555(5)
Ni2−O7	2.121(4)	P2−O6	1.526(5)
Ni2−O6B	2.006(4)	O7−C5	1.441(8)
O1−Ni1−O4	92.66(16)	O6B−Ni2−O2	176.45(16)
O1−Ni1−O1W	87.82(16)	O6B−Ni2−O5	97.31(17)
O4−Ni1−O1W	90.69(16)	O6B−Ni2−O7	92.11(16)
O2−Ni2−O5	84.55(17)	O6B−Ni2−O2W	92.28(17)
O2−Ni2−O7	85.12(16)	O6B−Ni2−O2C	96.97(17)
O2−Ni2−O2W	85.67(17)	P1−O1−Ni1	131.1(2)
O5−Ni2−O7	82.63(17)	P1−O2−Ni2	113.4(2)
O5−Ni2−O2W	169.67(17)	P1−O2−Ni2C	152.3(3)
O7−Ni2−O2W	93.23(17)	P2−O4−Ni1	136.6(3)
O2C−Ni2−O2	85.98(17)	P2−O5−Ni2	114.0(2)
O2C−Ni2−O5	91.83(18)	P2−O6−Ni2B	127.7(3)
O2C−Ni2−O7	169.91(17)	C5−O7−Ni2	103.4(3)
O2C−Ni2−O2W	90.81(17)	Ni2C−O2−Ni2	94.02(17)

[a] Symmetry codes: A, $-x+2$, $-y$, $-z+1$; B, $-x+1$, $-y$, $-z+2$; C, $-x+2$, $-y$, $-z+2$.

Table 4. Selected Bond Lengths (Å) and Angles (deg) for **3**

Co1−O1	2.050(4)	P1−O3	1.568(4)
Co1−O4	2.089(4)	P2−O4	1.507(4)
Co1−O1W	2.123(5)	P2−O5	1.502(4)
P1−O1	1.492(4)	P2−O6	1.571(4)
P1−O2	1.514(4)	O7−C5	1.429(6)
O1−Co1−O4	89.93(16)	P1−O1−Co1	135.0(2)
O1−Co1−O1W	84.77(17)	P2−O4−Co1	132.0(2)
O4−Co1−O1W	93.15(18)		

Table 5. Selected Bond Lengths (Å) and Angles (deg) for **4**

Ni1−O1	2.031(3)	P1−O3	1.568(3)
Ni1−O4	2.055(3)	P2−O4	1.498(4)
Ni1−O1W	2.074(4)	P2−O5	1.494(4)
P1−O1	1.487(3)	P2−O6	1.574(4)
P1−O2	1.503(4)	O7−C5	1.440(5)
O1−Ni1−O4	90.90(14)	P1−O1−Ni1	134.0(2)
O1−Ni1−O1W	93.73(14)	P2−O4−Ni1	132.6(2)
O4−Ni1−O1W	86.98(15)		

from the same ImhedpH$^-$ ligand, while the other three positions are filled with two phosphonate oxygens (O2C and O6B) from the other two equivalent ImhedpH$^-$ ligands and one water molecule (O2W). The Co−O bond lengths are in the range of 2.001(3)−2.180(3) Å, in agreement with those in $(NH_4)_2Co_2(hedpH)_2$, $[NH_3(CH_2)_nNH_3]Co_2(hedpH)_2\cdot 2H_2O$, and $[NH_3C_6H_4NH_3]Co_2(hedpH)_2\cdot H_2O$.[13]

The ImhedpH$^-$ molecule serves as a hexadentate ligand. It chelates and bridges Co1 and Co2 by using four phosphonate oxygens (O1, O2, O4, O5) and the hydroxyl oxygen O7, hence forming a trimer unit of $Co_3(ImhedpH)_2(H_2O)_4$. These trimers are connected by edge-sharing of the $\{Co(2)O_6\}$ octahedra, forming an undulating chain along the *c* axis, which contains a $\{Co_2O_2\}$ dimer unit. The Co2−O2−Co2C angle within this dimer is 92.75(12)°. The Co2···Co2C distance is 3.023 Å. The adjacent chains are fused through the coordination of the phosphonate oxygen atom (O6) from

(13) (a) Yin, P.; Gao, S.; Zheng, L.-M.; Xin, X.-Q. *Chem. Mater.* **2003**, *15*(16), 3233. (b) Zheng, L.-M.; Gao, S.; Yin, P.; Xin, X.-Q. *Inorg. Chem.* **2004**, *43*, 2151. (c) Yin, P.; Gao, S.; Wang, Z.-M.; Yan, C.-H.; Zheng, L.-M.; Xin, X.-Q. *Inorg. Chem.* **2005**, *44*, 2761.

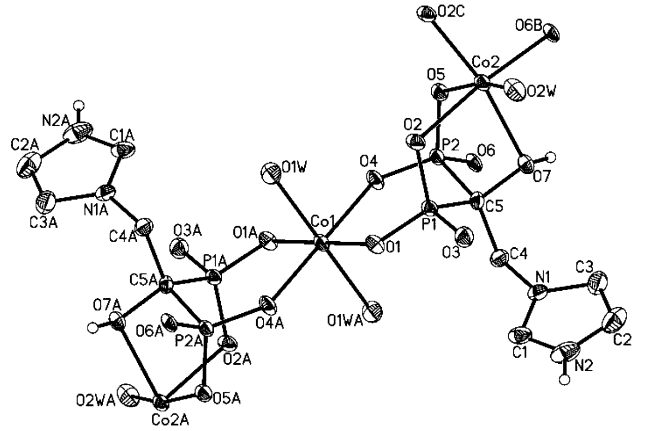

Figure 1. Trimer unit in **1** with atomic labeling scheme (50% probability). All H atoms except those attached to N2 and O7 are omitted for clarity.

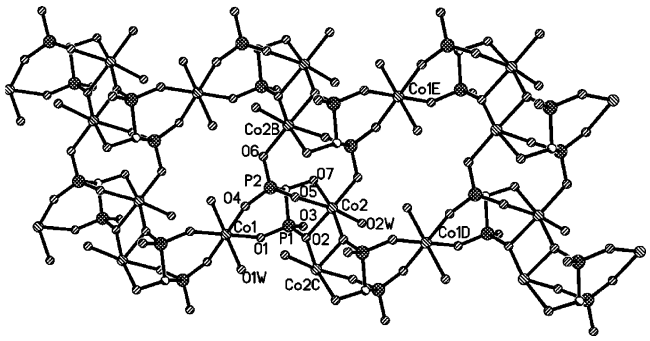

Figure 2. The inorganic layer of **1**. Symmetry codes: A, $-x+2$, $-y$, $-z+1$; B, $-x+1$, $-y$, $-z+2$; C, $-x+2$, $-y$, $-z+2$; D, x, y, $z+1$; E, $x-1$, y, $z+1$.

one chain to the Co(2) atom from the other, hence generating a two-dimensional layer containing 4-, 8-, and 16-membered rings (Figure 2). The remaining one phosphonate oxygen (O3) is protonated. The Co···Co distances across the O−P−O units are 5.372, 4.561, 4.859, and 6.336 Å for Co2···Co1, Co2···Co2B, Co2···Co1D, and Co2···Co1E, respectively.

The protonated imidazole groups protrude from two sides of the inorganic layer and are hydrogen bonded to the phosphonate oxygen O1 [N2···O1^{i} 2.723(6) Å] from the neighboring layer (Figure 3). Extensive hydrogen bonds are also observed among the coordinated and lattice water molecules as well as the phosphonate and hydroxy oxygen atoms. The O3W···O3, O3W···O2W, O2W···O1W^{ii}, O2W···O5^{ii}, and O7···O5^{iii} distances are 2.691(6), 2.749(6), 2.725(5), 2.817(5), and 2.607(4) Å, respectively (symmetry codes: i, $-x+2$, $-y+1$, $-z+1$; ii, $-x+2$, $-y$, $-z+2$; iii, $-x+1$, $-y$, $-z+2$). The interlayer separation is about 9.573(2) Å.

The structure of compound **2** is analogous to that of **1** except that the Co(II) ion in **1** is replaced by Ni(II) in **2**. The Ni−O bond lengths are in the range of 2.006(4)−2.121(4) Å, comparable to those in the other nickel phosphonate compounds such as $(enH_2)Ni(hedpH_2)_2\cdot 2H_2O$.[14] Within the layer, the Ni···Ni distance across the μ-O bridge is 3.001 Å, and those across the O−P−O units are 5.319 Å for Ni2·

(14) Song, H.-H.; Zheng, L.-M.; Lin, C.-H.; Wang, S.-L.; Xin, X.-Q.; Gao, S. *Chem. Mater.* **1999**, *11*, 2382.

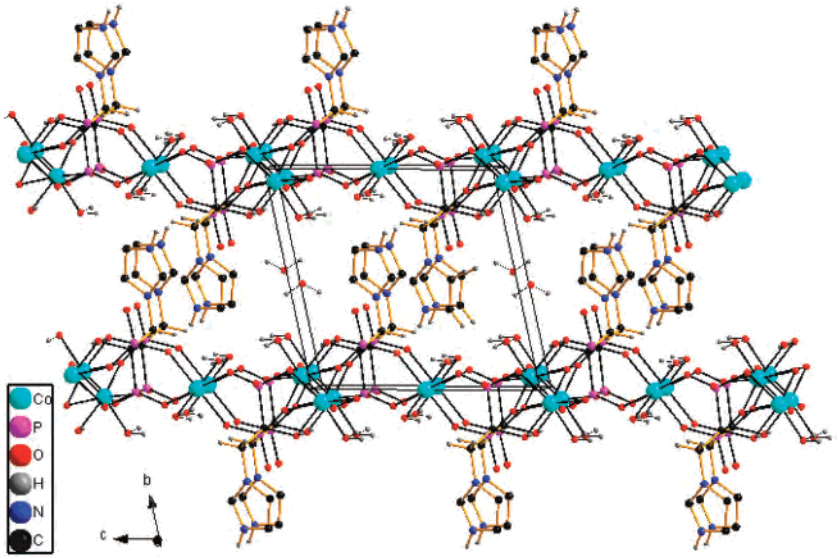

Figure 3. Packing diagram of structure **1** viewed approximately along the *a* axis. All H atoms except those attached to N and water molecules are omitted for clarity.

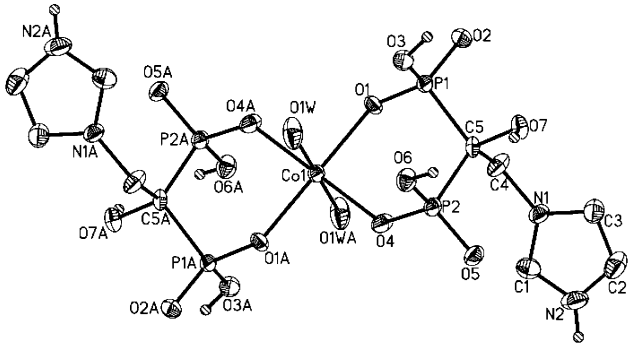

Figure 4. Mononuclear structure in **3** with atomic labeling scheme (50% probability). All H atoms attached to C are omitted for clarity.

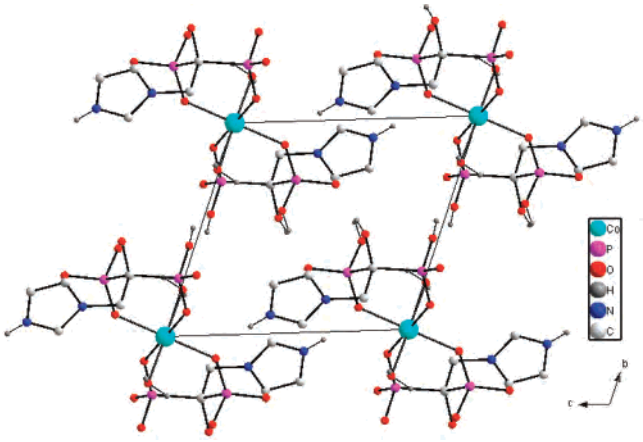

Figure 5. Packing diagram of structure **3** viewed along the *a* axis. All H atoms attached to C are omitted for clarity.

···Ni1, 4.538 Å for Ni2···Ni2B, 4.822 Å for Ni2···Ni1D, and 6.312 Å for Ni2···Ni1E, which are distances slightly shorter than the corresponding Co···Co distances in compound **1** due to the smaller ionic radii of the Ni(II) ion. The Ni2−O2−Ni2C bond angle is 94.02(17)°, larger than that in **1**. Extensive hydrogen bonds are also observed in **2**. The interlayer separation is about 9.625(3) Å. To the best of our knowledge, this type of layered structure has not been observed in the other metal diphosphonate compounds.

Crystal Structures of $M(ImhedpH_3)_2(H_2O)_2$ [M = Co-(II) (3), Ni(II) (4)]. Compounds **3** and **4** are isostructural. Each exhibits a mononuclear structure consisting of one M(II), two $ImhedpH_3^-$ ligands, and two coordination water molecules. Figure 4 shows the molecular structure of **3** with its atomic labeling scheme. The Co1 atom lies in an inversion center and has a slightly distorted-octahedral geometry. Two pairs of phosphonate oxygen atoms (O1, O4, O1A, O4A) from two equivalent $ImhedpH_3^-$ ligands define the equatorial plane, while two equivalent water molecules (O1W and O1WA) occupy the axial sites. The Co1−O bond lengths are 2.050(4)−2.123(5) Å. The O−Co1−O bond angles are 84.77(17)−95.23(17)°. Each $ImhedpH_3^-$ acts as a bidentate ligand and chelates to the Co1 atom by using phosphonate oxygen atoms O1 and O4. Two of the remaining four phosphonate oxygens are protonated [P1−O3 = 1.568(4) Å and P2−O6 = 1.571(4) Å]. An extensive hydrogen-bonding network is found among the phosphonate oxygens, hydroxyl groups, the protonated imidazole group, and water molecules, hence forming a three-dimensional supramolecular structure (Figure 5). The shortest O(N)···O distances are 2.592(6) Å for O3···O2^{ii}, 2.663(6) Å for O6···O5^{iii}, 2.871(6) Å for O7···O5^{iii}, and 2.713(7) Å for N2···O4^{iv} (symmetry code: ii, $-x+1, -y+1, -z$; iii, $-x+1, -y+1, -z+1$; iv, $-x+1, -y, -z+1$). Structure **4** is analogous to that of **3** except that the Co atoms are replaced by the Ni atoms.

Magnetic Properties of $Co_3(ImhedpH)_2(H_2O)_4\cdot 2H_2O$ (1). The temperature-dependent magnetic susceptibilities of compound **1** were investigated in the temperature range of 1.8−300 K. The room-temperature effective magnetic moment per Co_3 unit (8.78 μ_B) is much higher than the expected spin-only value for $S = {}^3/_2$ (6.71 μ_B), attributed to the orbital contribution of Co(II) ion. The susceptibility data between 90 and 300 K follows the Curie−Weiss law with a Weiss constant $\theta = -12.3$ K. Upon cooling from room temperature, $\chi_M T$ decreases continuously until it reaches a minimum of

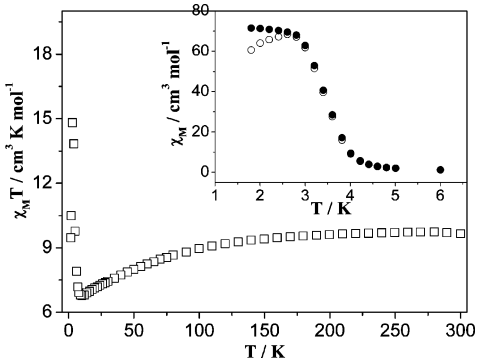

Figure 6. $\chi_M T$ vs T plot for **1**. Inset: ZFCM (○) and FCM (●) curves for **1**.

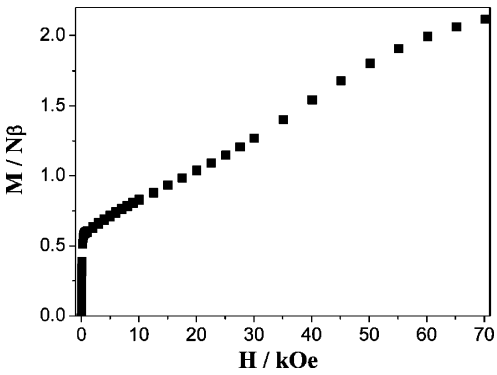

Figure 7. Field-dependent magnetization for **1** at 1.8 K.

6.78 $cm^3 \cdot K \cdot mol^{-1}$ at 10 K, $\chi_M T$ increases abruptly to a maximum of 14.82 $cm^3 \cdot K \cdot mol^{-1}$ at 3 K and then decreases again to 9.46 $cm^3 \cdot K \cdot mol^{-1}$ at 1.8 K (Figure 6). This is characteristic for a ferrimagnetic behavior with dominant antiferromagnetic interactions between the Co(II) ions. Besides, the zero-field-cooled magnetism (ZFCM) and field-cooled magnetism (FCM, $H_{dc} = 50$ Oe) measurements of the dc magnetic susceptibility deviate from each other at ca. 2.6 K, suggesting the onset of a long-range ferromagnetic phase transition below this temperature (Figure 6, inset).

The ferromagnetic transition is confirmed by the field-dependent isothermal magnetization M(H) performed at 1.8 K. As shown in Figure 7, an abrupt increase of magnetization to a value of ca. 0.57 Nβ is observed at 0.4 kOe. Between 0.4 and ca. 10 kOe, the magnetization shows a linear increase. When the external field is further increased, the magnetization experiences an S-shaped increase and approaches a value of 2.12 Nβ at 70 kOe (Figure 7). No magnetic hysteresis is present even at 1.8 K which classifies this material as a soft weak ferromagnet.

According to the structure of compound **1**, the Co(II) ions within the layer are bridged by μ-O and O−P−O units. Although the intralayer interactions through these exchange pathways are principally antiferromagnetic, the odd number of the Co(II) ions in the trimer unit of $Co_3(ImhedpH)_2(H_2O)_4$ leads to a nonzero net magnetic moment.[6,15] This corresponds to an intralayer ferromagnetic-like behavior as observed in **1**. For the Co(II) ion in an octahedral environment, an effective spin of $^1/_2$ with anisotropic g is usually expected at low temperature due to the overall effect of crystal-field and spin−orbit coupling.[16] Therefore, the ferromagnetic-like layer of $\{Co_3(ImhedpH)_2(H_2O)_4\}_n$ would result in one uncompensated $S = {}^1/_2$ spin, and a magnetization value of 2.1−2.5 Nβ would be anticipated with $g = 4.1-5.0$.[15,17]

Since the saturation value of magnetization at 0.4 kOe (0.57 Nβ per Co_3) is well below the expected value (M_S = 2.1−2.5 Nβ), the observed ferromagnetic-like ordering is attributed to canted antiferromagnetism (weak ferromagnetism) between the layers; i.e., perfect antiparallel alignment of the spins on neighboring metal ions between the antiferromagnetically coupled layers is not achieved, so residual spins are generated. The canting angle α is estimated to be 1.1° calculated from the expression $\sin(\alpha) = M_R/M_S$,[18] where M_R of 0.041 Nβ is deduced from the extrapolation of the linear portion of higher magnetic field and M_S of 2.1 Nβ is used. The magnetization value at 70 kOe (2.12 Nβ per Co_3) is close to the expected value of 2.1−2.5 Nβ, indicating a metamagnetic transition from a weak ferromagnetic state to a ferrimagnetic state. The critical field of this metamagnetic transition is ca. 38 kOe.

To obtain the critical temperature of the long-range magnetic ordering precisely, the zero-field ac magnetic susceptibility measurements were performed under $H_{ac} = 5$ Oe and a frequency of 1−499 Hz. Surprisingly, both the in-phase and out-of-phase signals, χ_M' and χ_M'', display a maximum which is strongly frequency dependent (Figure 8), implying a slow relaxation process. This slow relaxation process could be caused by either domain wall movements[19] or spin-glass behaviors.[20] The shift of the peak temperature (T_p) of χ_M' is measured by a parameter $\phi = (\Delta T_p/T_p)/\Delta(\log f) = 0.03$ (f is the frequency of H_{ac}), which is in the range of a normal spin-glass. The frequency dependence of T_p on χ_M'' can be fitted well to the Arrhenius law: $\tau(T) = \tau_0 \exp(\Delta/k_B T)$, where τ_0 is the pre-exponential factor and Δ is the energy gap. The best fit results in parameters $\tau_0 = 1.2 \times 10^{-10}$ s and $\Delta/k_B = 46$ K. The activation energy may be compared with those typical for the domain wall movements.[19]

Magnetic Properties of $Ni_3(ImhedpH)_2(H_2O)_4 \cdot 2H_2O$ (2). The magnetic behavior of compound **2** is analogous to that of compound **1**. The room-temperature effective magnetic moment per Ni_3 unit (5.60 μ_B) is close to the expected value

(15) (a) Drillon, M.; Coronado, E.; Belaiche, M.; Carlin, R. L. *J. Appl. Phys.* **1988**, *63*, 3551. (b) Konar, S.; Mukherjee, P. S.; Zangrando, E.; Floret, F.; Chaudhuri, N. R. *Angew. Chem., Int. Ed.* **2002**, *41*, 1561.

(16) (a) Jankovics, H.; Daskalakis, M.; Raptopoulou, C. P.; Terzis, A.; Tangoulis, V.; Giapintzakis, J.; Kiss, T.; Salifoglou, A. *Inorg. Chem.* **2002**, *41*, 3366. (b) Rujiwatra, A.; Kepert, C. J.; Claridge, J. B.; Rosseinsky, M. J.; Kumagai, H.; Kurmoo, M. *J. Am. Chem. Soc.* **2001**, *123*, 10584. (c) Caneschi, A.; Dei, A.; Gatteschi, D.; Tangoulis, V. *Inorg. Chem.* **2002**, *41*, 3508.

(17) Robinson, W. K.; Friedberg, S. A. *Phys. Rev.* **1960**, *117*, 402.

(18) Wang, X.-Y.; Gan, L.; Zhang, S.-W.; Gao, S. *Inorg. Chem.* **2004**, *43*, 4615.

(19) (a) Bellouard, F.; Clemente-León, M.; Coronado, E.; Galán-Mascarós, J. R.; Gómez-García, C. J.; Romero, F.; Dunbar, K. R. *Eur. J. Inorg. Chem.* **2002**, 1603. (b) Coronado, E.; Gómez-García, C. J.; Nuez, A.; Romero, F. M.; Rusanov, E.; Stoeckli-Evans, H. *Inorg. Chem.* **2002**, *41*, 4615.

(20) Mydosh, J. A. *Spin Glasses: An Experimental Introduction*; Taylor & Francis: London, 1993.

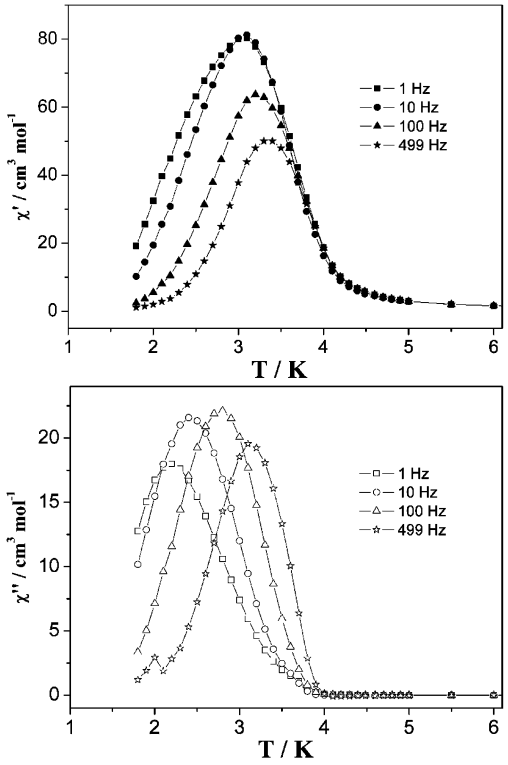

Figure 8. Temperature dependence of zero-field ac magnetic susceptibility for **1**.

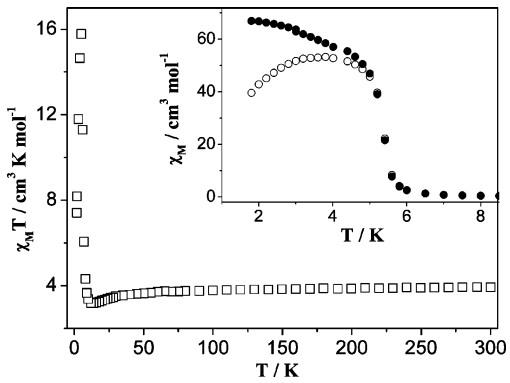

Figure 9. $\chi_M T$ vs T plot for **2**. Inset: ZFCM (○) and FCM (●) curves for **2**.

(5.38 μ_B) for spin $S = 1$ with $g = 2.2$. Upon cooling from room temperature, the $\chi_M T$ value decreases from 3.92 to 3.17 $cm^3 \cdot K \cdot mol^{-1}$ at ca. 14 K, below which it increases rapidly to a maximum of 15.78 $cm^3 \cdot K \cdot mol^{-1}$ at 5 K and then decreases again to 7.40 $cm^3 \cdot K \cdot mol^{-1}$ at 1.8 K (Figure 9). This is typical for ferrimagnetic behavior. The FCM (H_{dc} = 50 Oe) and ZFCM curves diverge at ca. 5.0 K (Figure 9, inset), suggesting that a long-range magnetic ordering occurs below $T_c = 5.0$ K. The isothermal magnetization M(H) at 1.8 K reveals that the magnetization at 70 kOe (0.86 Nβ) is far below the saturation value of 2.2 Nβ expected for an S = 1 system ($g = 2.2$), indicating the occurrence of canted antiferromagnetism. The magnetic hysteresis loop is observed at 1.8 K with the coercive field (H_c) and the remnant magnetization (M_R) being 22.5 Oe and 0.098 Nβ, respectively (Figure 10). The canting angle is estimated as 2.6°.

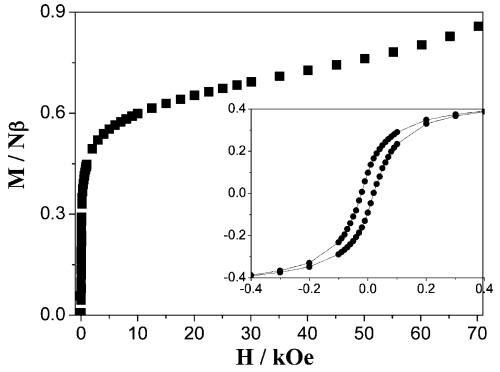

Figure 10. Field-dependent magnetization and hysteresis loop (inset) for **2** at 1.8 K.

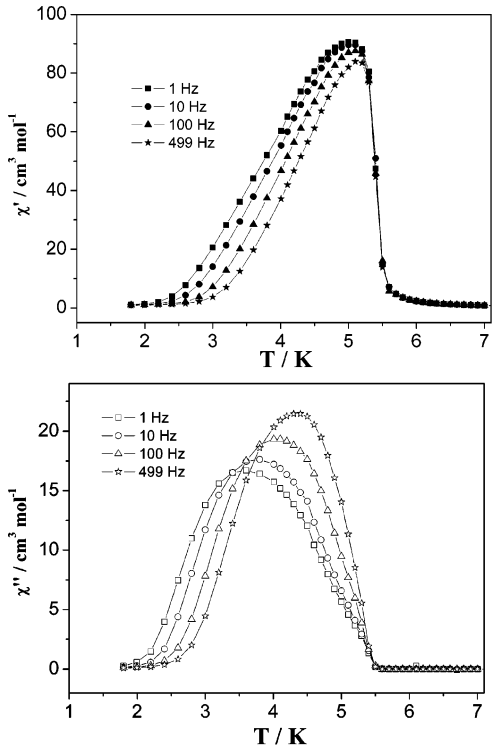

Figure 11. Temperature dependence of zero-field ac magnetic susceptibility for **2**.

The zero-field ac magnetic susceptibility measurement under $H_{ac} = 5$ Oe and a frequency of 1−499 Hz shows both in-phase and out-of-phase signals that are strongly frequency dependent (Figure 11). The shift of the peak temperature (T_p) of χ_M' is measured by a parameter $\phi = (\Delta T_p/T_p)/\Delta(\log f) = 0.01$ which is in the range of a spin-glass. The relaxation time (τ) may be calculated from the Arrhenius law, leading to parameters $\tau_0 = 2.1 \times 10^{-17}$ s and $\Delta/k_B = 131$ K. The activation energy is comparable to those typical for the domain wall movements,[19] although the τ_0 value is too small.

Canted antiferromagnetism, caused by an antisymmetrical component of the superexchange interaction (Dzyaloshinsky-Moriya interaction) and also by single ion anisotropy,[21] has already been found in a few other cobalt or nickel phosphonate compounds including $\{K_2[CoO_3PCH_2N(CH_2CO_2)_2]\}_6 \cdot$

(21) Carlin, R. L. *Magnetochemistry*; Springer: Berlin, 1986; pp 149−152.

xH_2O,[22] $Co_3(O_3PC_2H_4CO_2)_2$,[23] and $Ni\{CH_3(CH_2)_{17}PO_3\}(H_2O)$.[24] The observation of canted antiferromagnetism in **1** and **2** is not unexpected due to the unsymmetrical exchange couplings between the neighboring metal ions. However, the coexistence of the slow relaxation process in a layered cobalt or nickel phosphonate compound is unusual. This relaxation process could be due to the spin-glass behaviors and/or domain wall movements. The small ϕ values obtained from the frequency dependence of T_p on χ_M' support a spin-glass behavior in both **1** and **2**, while the activation energies obtained from the frequency dependence of T_p on χ_M'' suggest the presence of domain wall movements. Apparently, compounds **1** and **2** show quite unusual magnetic behaviors and are tentatively ascribed to the canted antiferromagnet with spin-glass-like relaxation. Since the randomness (defects, disorder, etc.) and frustration (geometrical or competitive) are responsible for the spin-glass system,[20] the spin-glass-like behavior of compounds **1** and **2** could be related to the possible crystal defects and/or the presence of some degree of frustration caused by the triangle arrangement of the cobalt(II) ions linked by three phosphonate oxygen atoms (Co1, Co2, and Co2B, for instance) in the magnetic lattice. Weak ferromagnetism with slow relaxation behavior has already been observed in a few coordination polymers including $[Ni(\mu\text{-}N_3)(bmdt)(N_3)](DMF)$ [bmdt = *N*,*N*′-bis(4-methoxylbenzyl)-diethylenetriamine and DMF = dimethylformamide][25] and $[Co_3(DMF)_{12}][W(CN)_8]_2$[26] with chain structures, $[Ni(C_6H_{14}N_2)_2]_3[Fe(CN)_6]_2\cdot 2H_2O$ with a layer structure,[19] and $[Co_4(2\text{-mna})_4(OH_2)]$ (2-mna = 2-mercaptonicotinate) with a three-dimensional structure.[27]

Conclusions

By the use of zoledronic acid, compounds $M_3(ImhedpH)_2(H_2O)_4\cdot 2H_2O$ [M = Co(II) (**1**) and Ni(II) (**2**)] with a novel type of layer structure and compounds $M(ImhedpH_3)_2(H_2O)_2$ [M = Co(II) (**3**) and Ni(II) (**4**)] with a mononuclear structure have been prepared under hydrothermal conditions. Both **1** and **2** show canted antiferromagnetism at 2.6 and 5.0 K, respectively, below which spin-glass-like relaxation behavior is observed. As far as we know, these are the first examples of metal phosphonates that exhibit the coexistence of weak ferromagnetism and relaxation behaviors. Further work is in progress to explore materials with new topologies and interesting magnetic properties based on the related diphosphonate ligands involving different functional groups.

Acknowledgment. We thank the National Natural Science Fund for Distinguished Young Scholars (No. 20325103), the NSF fund (No. 20631030), and the specialized research fund for the doctoral program of the Ministry of Education of China (No. 20040284004) for financial support. We also thank Profs. S. Gao and Y. Song for valuable discussions.

Supporting Information Available: X-ray crystallographic files in CIF format for the four compounds; $\ln(2\pi f)$ vs $1/T$ plots for compounds **1** and **2** in PDF format. This material is available free of charge via the Internet at http://pubs.acs.org.

IC701098T

(22) Gutschke, S. O. H.; Price, D. J.; Powell, A. K.; Wood, P. T. *Angew. Chem., Int. Ed.* **1999**, *38*, 1088.
(23) Rabu, P.; Janvier, P.; Bujoli, B. *J. Mater. Chem.* **1999**, *9*, 1323.
(24) Bellitto, C.; Bauer, E. M.; Ibrahim, S. A.; Mahmoud, M. R.; Righini, G. *Chem.—Eur. J.* **2003**, *9*, 1324.
(25) Liu, X.-T.; Wang, X.-Y.; Zhang, W.-X.; Cui, P.; Gao, S. *Adv. Mater.* **2006**, *18*, 2852.
(26) Li, D.-F.; Zheng, L.-M.; Zhang, Y.-Z.; Huang, J.; Gao, S.; Tang, W.-X. *Inorg. Chem.* **2003**, *42*, 6123.
(27) Humphrey, S. M.; Alberola, A.; García, C. J. G.; Wood, P. T. *Chem. Commun.* **2006**, 1607.